Lab on a Chip
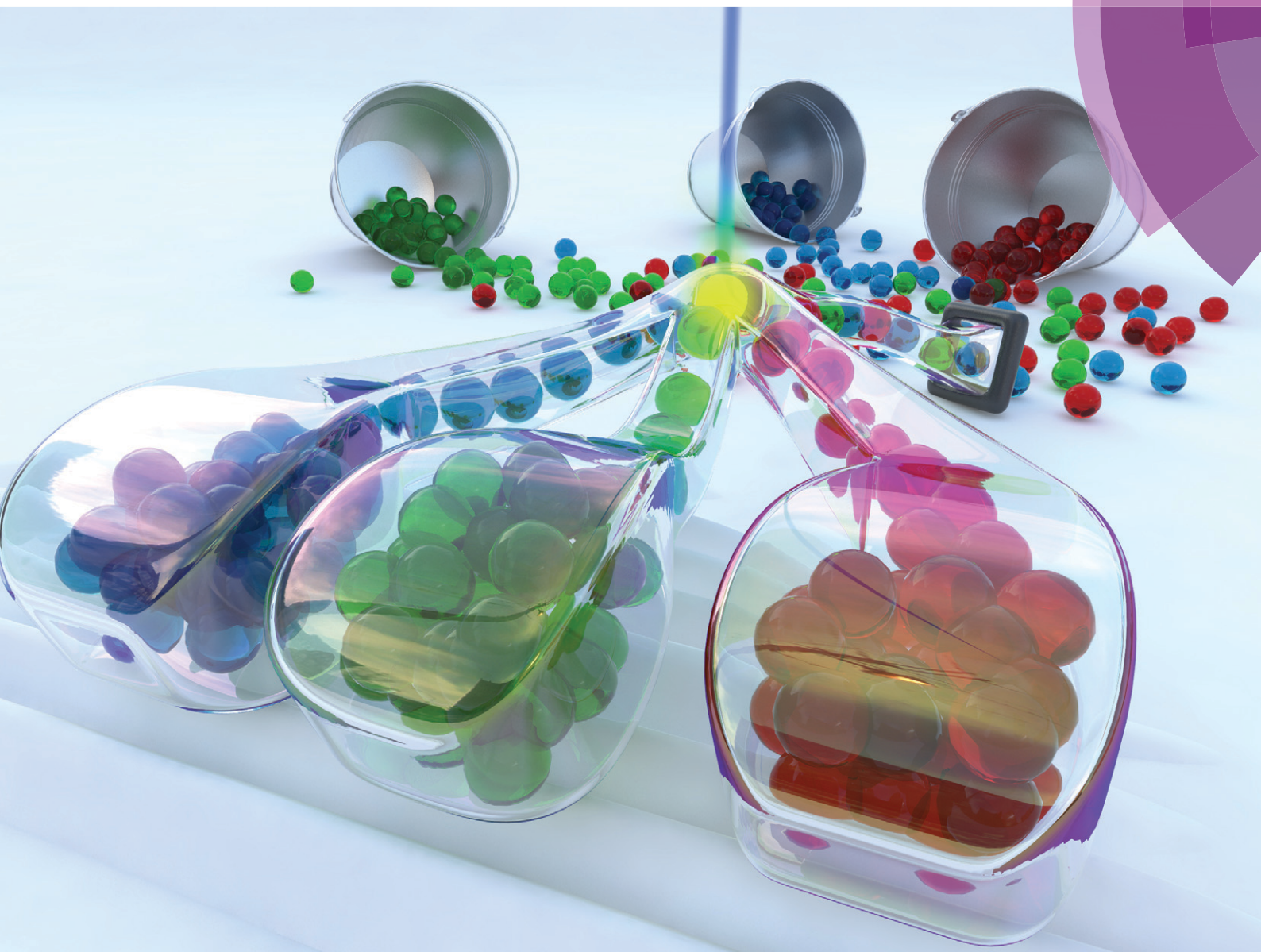
Miniaturisation for chemistry, physics, biology, materials science and bioengineering

ROYAL SOCIETY OF CHEMISTRY

PAPER
Thomas Franke *et al.*
Sorting drops and cells with acoustics: acoustic microfluidic
fluorescence-activated cell sorter

Sorting drops and cells with acoustics: acoustic microfluidic fluorescence-activated cell sorter†

Lothar Schmid,[a] David A. Weitz[b] and Thomas Franke*[abc]

We describe a versatile microfluidic fluorescence-activated cell sorter that uses acoustic actuation to sort cells or drops at ultra-high rates. Our acoustic sorter combines the advantages of traditional fluorescence-activated cell (FACS) and droplet sorting (FADS) and is applicable for a multitude of objects. We sort aqueous droplets, at rates as high as several kHz, into two or even more outlet channels. We can also sort cells directly from the medium without prior encapsulation into drops; we demonstrate this by sorting fluorescently labeled mouse melanoma cells in a single phase fluid. Our acoustic microfluidic FACS is compatible with standard cell sorting cytometers, yet, at the same time, enables a rich variety of more sophisticated applications.

Introduction

Fluorescence-activated cell sorting (FACS) is a widely used technology that is a critical tool in molecular biology, genetics and immunology.[1,2] It is often used to select subpopulations of cells from a large number of cells in drug screening and diagnostics and has developed into a commercially available standard technique. It also has great potential for emerging biotechnologies such as systems biology, rare cell detection or stem cell isolation.

FACS uses laser interrogation based on fluorescence or scattering to identify single cells followed by the encapsulation of cells in drops that form an aerosol and that are sorted at very high rates through application of an electric field.

Many operational and technical difficulties associated with cell sorting arise in auxiliary operations. Cells growing in culture must be sterile to maintain their viability. Practical procedures to ensure the quality of the sorted sample are both time-consuming and costly; for example, RNase-free processing entails sterilization and cleaning of the complete tubing and filter system of the FACS machine, requiring considerable time. Moreover, because of the high acquisition cost of commercial FACS machines, cell sorting service is generally offered by central facilities.

Microfluidics technologies enable affordable, desk-top-scale platforms suitable for individual lab use. The sample chambers

are disposable, eliminating the need for complex cleaning and sterilization, and consume very low volumes of reactants. In addition, efforts to provide a biosafety environment to handle potentially biohazardous materials are greatly reduced because the sample is always self-contained and aerosol production is eliminated; thus, operation in a hood or biosafety lab is typically not required.

However, realizing a microfluidic fluorescence actuated cell sorter still remains challenging because microfluidic actuation and deflection mechanisms of cells are slow and inflexible. Many devices exploit dielectrophoretic forces that depend on the volume and dielectric contrast of the sorted objects and the continuous medium.[3] Yet, to osmotically balance the cytosol, cells are suspended in cell buffer media that possess a low dielectric contrast as the cells and which cannot be replaced with a high-contrast agent. Similarly, magnetic actuated sorting suffers from dependence on magnetic susceptibility contrast and is also volume dependent. Recently, acoustic radiation forces in a gradient of a standing acoustic wave field have been used to deflect cells,[4–10] but in this approach the forces depend on both compressibility contrast and cell size. All of these actuation mechanisms critically depend on the volume of the objects and small objects are inherently more difficult to sort. This also makes it difficult to sort cell populations that have a wide distribution of sizes.

In this way a low and size-dependent deflection force also results in slow sorting rates. Methods for enhancing sorting forces are limited. To overcome this drawback, other techniques have been employed: immunopolystyrene beads are used to selectively bind to target cells, both to label cells and to enhance sorting by increasing their effective dielectric or paramagnetic contrast.[11,12] Alternatively, cells can be encapsulated into fluid containers or drops that provide sufficient contrast with the continuous fluid.[13–15] Yet, both methods require the

[a] *Lehrstuhl für Experimentalphysik I, Soft Matter Group, Universität Augsburg, Universitätsstr. 1, 86159 Augsburg, Germany. E-mail: Thomas.Franke@glasgow.ac.uk*
[b] *Department of Physics and School of Engineering and Applied Science, Harvard University, 29 Oxford Street, Cambridge, Massachusetts 02139, USA*
[c] *Chair of Biomedical Engineering, School of Engineering, College of Science and Engineering, University of Glasgow, Rankine Building, Oakfield Avenue, G12 8LT, UK*
† Electronic supplementary information (ESI) available. See DOI: 10.1039/c4lc00588k

addition of supplemental additives, either beads or immiscible fluid, to achieve sorting. Another alternative is the use of fluid-switching techniques which do not depend on volume or contrast.[16–19] Instead, they employ fluid valves that direct the fluid flow into a collection channel. However, these techniques suffer from a low response time, limiting switching rates to a few hundreds per second.

In this paper, we overcome the limitations of the commonly used microfluidic sorting techniques using actuation by using travelling surface acoustic waves. These have been used previously for mixing and moving droplets on a substrate,[20] lysing cells,[21] and mixing in microfluidic channels[22] as well as particle concentration[23] and fluid nebulization,[24] employing the acoustic streaming effect. Travelling waves have also been used to generate an acoustic radiation force on particles, which is size dependent and allows for size separation and filtering. While the acoustic radiation force depends on particle volume and acoustic impedance contrast,[7] acoustic streaming actuates particles independent of their properties[25–27] and is therefore particularly useful for small particles.

We introduce an acoustic sorting technique that is able to sort cells and other objects at high rates and independent of their size or contrast, which is important for bacteria and virus sorting. In our microfluidic device we select and deflect cells and objects directly from the bulk solution without enhancement with responsive labels or other additives which introduce sample contamination. Cells that are interrogated using laser-based detection are sorted by acoustic actuation using a surface-acoustic wave device into two, or even more, collection channels, enabling simple parallelization. The response times are very short and switching rates of the electronically controlled acoustic actuation are extremely fast. Our method offers all of the advantages of microfluidic devices, such as low cost and sample volume, while requiring small fluid volumes and using disposable sample cells, simplifying sample cleaning and preparation.

Experimental results and discussion

We sort using acoustic actuation and deflection based on the level of an interrogation signal. Our acoustofluidic hybrid device for sorting combines conventional soft lithography with surface acoustic wave technology (SAW) to drive microflows. To generate a SAW on the chip we use interdigitated transducers (IDT). We vapor deposit those comb-like electrodes on a transparent piezoelectric substrate made of lithium niobate and generate a mechanical acoustic wave by applying a high-frequency electric signal to the IDT. SAWs excited in this way typically propagate at very low attenuation along the substrate surface. However, if we deposit a fluid such as water on top of the substrate the surface wave gets strongly attenuated and the acoustic energy couples into the fluid. The momentum of the refracted wave which enters the fluid in this way gives rise to an acoustic streaming of the fluid.[28] We exploit this effect to deflect and sort the sample in microfluidic channels as shown in Fig. 1 (see also the ESI† Movie 1).
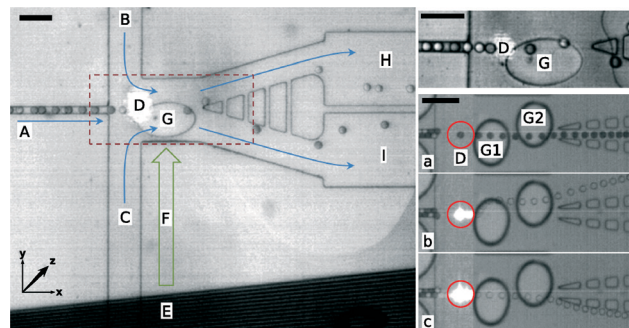

Fig. 1 (left) Top view of the droplet sorter setup. The droplets enter the sorting device through the inlet channel A. The top and bottom focusing channels B and C focus the droplets towards the middle of the channel to direct the droplets into the lower default outlet I. If a droplet passing the interrogation region D emits a fluorescence signal, a surface acoustic wave (SAW) is generated by the interdigitated transducer E, travelling along a narrow path F towards the contact post G, where the resulting sound field directs the droplet upwards into the upper outlet H. (top right) Zoom view of the two-way droplet sorter. (bottom right) Top view of a triple sorting setup. An additional middle outlet was added to the setup, and the contact post was split into two staggered posts G1 and G2. Depending on the fluorescence intensity detected at the laser spot D, either the SAW is not activated at all (no fluorescence, a), or the SAW is directed towards post 1 or 2 (low or high fluorescence, b and c, respectively). In the first case, the droplets move towards the middle default outlet. If one of the post is activated, the droplets are pushed away from the center of the staggered posts, either upwards by the lower post (G1) or downwards by the higher one (G2), and into the respective sorting outlets. The droplets experience a force along the gradient of the acoustic intensity, which is higher on the posts than in the surrounding region. Images (a, b, c) are montages, each showing a single droplet moving through the sorting channel. The left part of the image shows the droplet in the center of the laser spot, the right part is an overlay of multiple images with a frame rate of dt = 0.3 ms, showing the droplet trajectory. Scale bars: 100 μm. Also see movie in the ESI.†

We fabricate the microfluidic device using a polydimethylsiloxane (PDMS) molding process and attach it to a thin PDMS layer of a few micrometers thick to form a sealed and closed microchannel device. The PDMS film features a small post that is carefully aligned below the sorting region of the microchannel. To accomplish the hybrid device the sealed PDMS mold is then adjusted on top of the piezo-substrate with the sorting region close to the IDT to enhance optimal coupling of the acoustic energy into the fluid as shown in Fig. 2. This enables us to couple the acoustic wave into the microfluidic channel at a precise location.[25] Alternative methods have employed a single-layer device attached directly to the substrate; however, these methods lead to a more complex flow profile with several counter-rotating vortices[22,26] and generally provide less control of the acoustic path. The design of the microfluidic channels contains a sample inlet and a sheath flow for hydrodynamic focusing of the sample before sorting into two or more outlets. By controlling the sheath flow rate, sorting errors are prevented because drop separation can be optimized to ensure that only one drop appears at once in the sorting region. Furthermore, using slightly asymmetric flows, we calibrate the flow
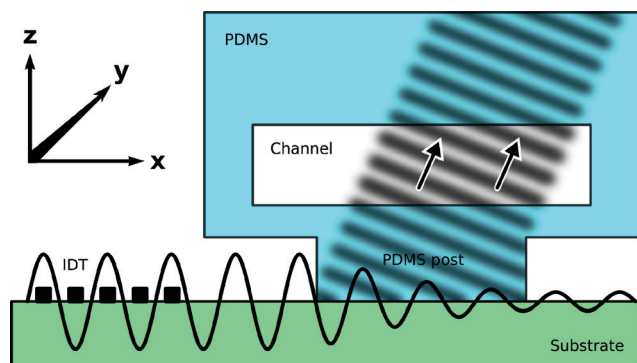
Fig. 2 Working principle of the surface acoustic wave (SAW) actuation (side view): the SAW is generated by an interdigitated transducer (IDT) on the chip. It travels along the chip surface towards the PDMS channel. In the region where the PDMS post is in contact with the chip surface, the surface wave is attenuated and a bulk sound wave couples to the PDMS and subsequently to the fluidic channel at an angle of 21.8°. The bulk wave in the fluid generates an acoustic radiation force on the droplets (in the case of oil emulsion droplets) or actuates the liquid *via* acoustic streaming (in the case of cells in aqueous solution) as indicated by the arrows.

conditions to align the sample trajectory and guide it into the waste channel in the absence of acoustic actuation. Careful alignment of the trajectory is also important to make sure that the sample flow passes through the center of the optical interrogation spot that detects the trigger signal for sorting. To optionally control the spacing between objects and to meet the specific requirements of the sample, we added another side channel further upstream to dilute the concentration of the sample. This is particularly useful to prevent the fluid shear stress-induced coalescence of densely packed drops when sorting at extreme speeds. To enhance the robustness of the sorter and maintain the balanced flow conditions, we introduce shunts between the two outlet channels to decouple the acoustic sorting region from any pressure disturbances further downstream in the micro-fluidic device that affect the hydrodynamic outlet resistance. Such pressure fluctuations do arise when there are variable numbers of drops in the collect and waste channels or simply when connecting tubing for sample collection.

We trigger the sorting on the level of a fluorescence signal of the sample in the interrogation area of a focused laser spot. The fluorescence signal is detected with a photo-multiplier tube and analyzed in real time. If the intensity of the fluorescence signal exceeds a preset threshold we trigger a high-frequency generator to send a pulse to the IDT to excite a SAW on the hybrid chip to diverge the sample.

We demonstrate fluorescence-activated droplet sorting using picoliter-volume aqueous drops dispersed in a continuous fluorocarbon oil phase that is stabilized with a biocompatible surfactant.[29] We produce fluorescent and non-fluorescent drops in a separate PDMS drop-maker device[30] and mix both populations. To enable optical discrimination and control of sorting in a transmitted light microscope we added the stain bromophenol blue to the non-fluorescent drops to blacken

them as shown in Fig. 1. The monodisperse mixture of drops is reinjected into the high-speed acoustic sorter at a high volume ratio. The drops then flow into a constriction to force them into a single file line. This facilitates timing and prevents coincidence of drop occurrence in the interrogation or sorting region that potentially causes false sorts. Dense packing of drops allows for the precise control of their flow rate by carefully tuning the sheath flow *via* the side channels. We select drops based on a preset fluorescence intensity threshold and acoustically direct them into the select channel.

Using this acoustofluidic hybrid device, we are able to sort drops at rates of several kHz.

The sorting speed depends on the duration required for the interaction between the drop and the acoustic field and the intensity of the acoustic wave power. Therefore, the maximum sorting rate of the sorter is limited by the minimum duration of the sorting pulse t_{pulse}. If the pulse is shorter, the deflection will not be sufficient to move the droplet to the collect channel. Furthermore, the droplet is only deflected during the time it is traveling through the actuation region above the post t_{act}. For optimal performance t_{act} is adjusted to t_{pulse} by carefully tuning the sheath flow rate. To sort consecutive droplets independently, only one droplet can be in the actuation region at once. Therefore the droplet separation time must be adjusted to $t_{sep} = t_{pulse}$. For non-aligned particles like cells in bulk fluid, the number of particles in the actuation region is Poisson distributed, which necessitates a trade-off between sorting rate and sorting yield and purity. However, when sorting droplets in a single file the edge-to-edge alignment in our droplet sorter eliminates this problem, allowing for adjustment of t_{sep} with a very low standard deviation. In our experiments, a minimum of $t_{sep} = 330$ μs with perfect sorting can be achieved, corresponding to a sorting rate of 3000 cells per second at a moderate SAW power of 15 dBm (see also section sorter performance).

This acoustic sorting principle in PDMS channels is not restricted to sorting into only one collection channel but is easily extended to sort drops into multiple outlet channels to separate a more complex population of drops. To demonstrate this versatility and flexibility of the device we sort drops into three categories. Here, we use two populations of fluorescence-labeled droplets with different fluorescence intensities in addition to a third population of non-fluorescent drops. The design of the channel was customized by adding a third outlet as well as a second PDMS post as shown in Fig. 1 (a–c). Non-fluorescent droplets are not actu-ated and drift into the central waste outlet. Fluorescent drop-lets are sorted either into the upper or into the lower outlet channel depending on their fluorescence intensity. We use tapered IDTs that allow us to selectively couple the acoustic wave either through the right (upper) or through the left (lower) post, thereby driving the droplets either up or down, respectively.

The applicability of our acoustic device is not only limited to guiding and sorting droplets but also enables direct manipulation of cells suspended in cell buffer media without

prior encapsulation and formation of drops. This procedure is similar to the fluid handling of commercial FACS machines that use only a single fluid.

We demonstrate acoustic cell sorting for B16F10 mouse melanoma cells. These cells are highly invasive and metastatic and are used in cancer research to screen drugs that reduce tumor growth[31] and inhibit metastasis.[32,33] To enable identification with our detector before sorting, the cells were treated with Calcein-AM, a fluorescence dye that is sensitive to cell metabolic activity and plasma membrane integrity.[34,35] This preparation yields a cell population with varying fluorescence intensity. To regulate the sorter we set a fluorescence intensity threshold. For sorting, cells suspended in phosphate-buffered saline (PBS) were injected into the sample inlet and aligned by a co-flowing sheath flow containing the same PBS solution. The sample flow is forced to form an extended fluid jet that aligns the cells as shown in Fig. 3.

In contrast to droplet sorting, a constant cell rate cannot be achieved since cells cannot be densely packed. They tend to form clusters caused by mutual adhesion and conglutination. In exactly the same way as in sorting with commercial FACS machines, the number of cells in the sorting region is therefore Poisson distributed. However, the mean rate can be regulated by adjusting cell concentration, sample flow rate and sheath flow rate.

Theory of acoustic streaming

The dissipation of a sound wave in a medium leads to an acoustic force that generates acoustic streaming of fluids in the same direction as the propagation. An acoustic wave with intensity $I_{ac}e^{-\beta x}$ (with initial intensity I_{ac} and attenuation coefficient β) that propagates in the x-direction at velocity c carries a momentum flux $I_{ac}c^{-1}e^{-\beta x}$ and permanently loses momentum over the attenuation length β^{-1}. Therefore, momentum conservation implies an exchange of momentum from the attenuated wave to the fluid. This gives rise to a volume force acting on the fluid[36]

$$F = \beta c^{-1}I_{ac}e^{-\beta x}$$

that can be considered as an external bulk force in the equation of motion for the fluid, with $\beta^{-1} = 975$ μm for water.[37]

Commonly, in microfluidics the equation of motion reduces to the non-inertial Stokes equation. However, acoustics is one of the few effects in microfluidics where inertial terms have to be explicitly taken into account. The actuation mechanism of acoustic streaming is evoked by an exchange of momentum that is inherently an inertial effect. Moreover, in our sorting device acoustic streaming induces a flow velocity component perpendicular to the syringe-driven flow direction in the microchannel. For discontinuous changes of flow direction, inertia effects become increasingly important, as can be observed at sharp corners in a channel. Therefore, to describe the fluid flow we have to consider the full Navier–Stokes equation in our simulations. (For a detailed discussion and comparison of inertia and non-inertia flows see ESI† discussion 1: inertial effects and Fig. S1.)

Simulations and experiments

To quantitatively model the acoustic flow field and acoustic streaming we simulate the effect of the surface acoustic wave (SAW) on the flow field in the microchannel using COMSOL Multiphysics (version 4.2a) and consider the full Navier–Stokes equation. We model a stationary laminar flow of an incompressible fluid and account for the acoustic streaming using a volume force calculated from the intensity profile of the SAW on the chip surface. The propagation direction of the wave (and therefore the direction of the force) is along the yz-plane tilted by a Rayleigh angle of 21.8° with respect to the z axis.

For comparison, the flow field has also been measured experimentally using particle image velocimetry (PIV). As shown in Fig. 4d, e, our simulations reproduce the key features of the experimental velocity field quite well. Both experimentally observed vortices in Fig. 4e are obtained from the simulations and agree quantitatively with the measured size and position. The distances between the vortex centers compare well, and the value and direction of velocity are also
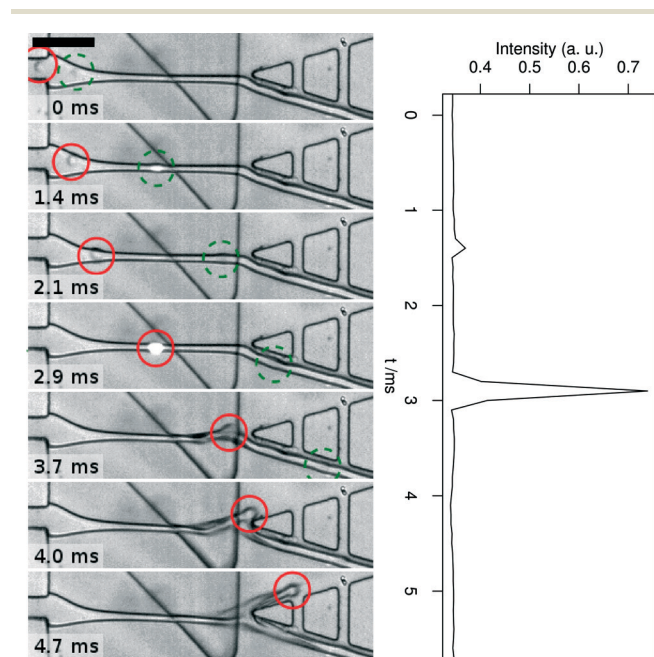

Fig. 3 (left) Top view of a cell sorting experiment. Mouse melanoma cells (B16F10) are treated with a stain sensitive to metabolic activity (Calcein–AM). The cells travel along the channel center and their fluorescence is measured in the laser spot and are subsequently deflected when passing the post, which is triangular in this setup. The plot on the right shows the fluorescence peaks of the two cells. The first cell (green dashed circle) has low fluorescence and is therefore not deflected, flowing into the waste channel. The second cell (red circle) has high fluorescence which triggers the sorter, deflecting the cell into the collect channel. Scale bar: 100 μm. (right) Plot of the fluorescence intensity at the laser spot showing the fluorescence peaks of the two cells at $t = 1.4$ ms and $t = 2.9$ ms, respectively.
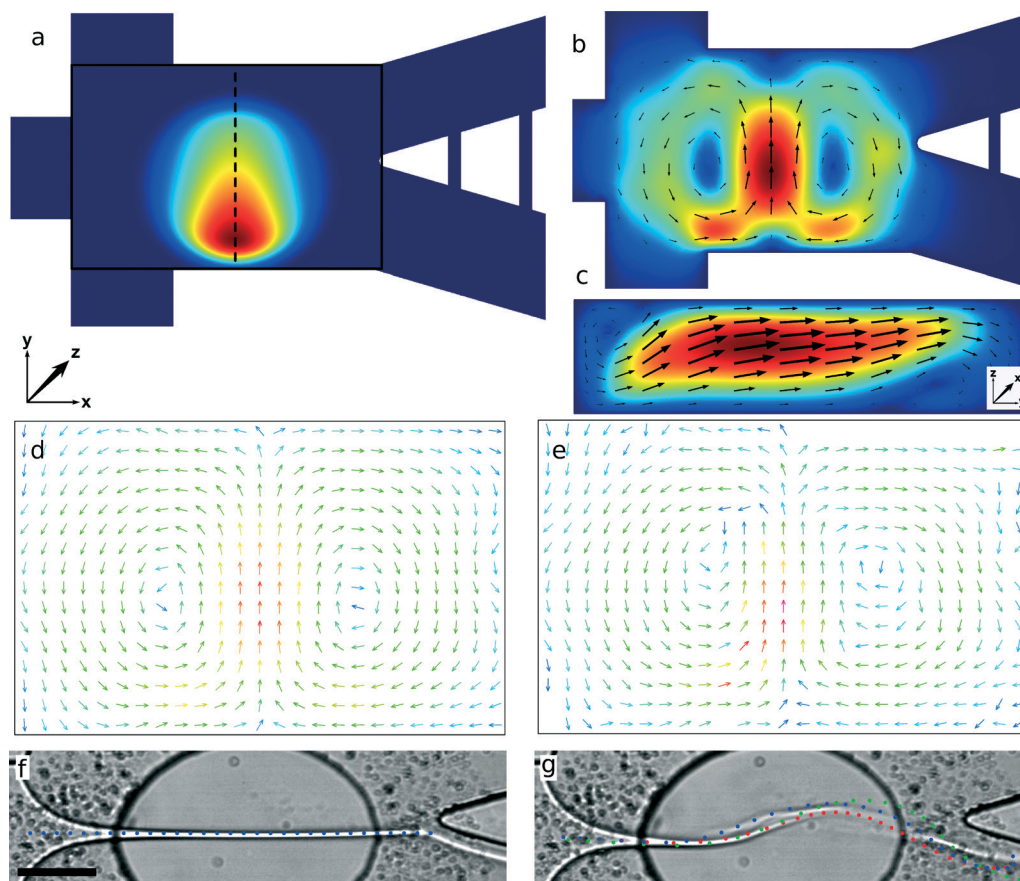
Fig. 4 (a) Top view of the simulation. The color plot shows the actuating volume force acting above the post, which is dampened in the y-direction. The colored line shows the vertical section along the yz-plane that is plotted below. The rectangle shows the region of the comparison plot d and e. (b) Top view of the simulation showing the xy-velocity along a mid-plane section of the channel. A strong central stream bifurcates into two backflow arms, generating a double vortex. (c) Side view of the simulation (section along the yz-plane) showing in-plane velocity. Due to geometric constraints, the flow is mainly in the y-direction even though the force is predominantly in the z-direction (at a Rayleigh angle of 21.8°). (d, e) A comparison of simulations (d) and PIV measurements (e) of the flow field in the sorting region is in good agreement with the distance of the two vortices as well as a high velocity in the middle (above the post) and a lower velocity in the backflow region. Velocities are normalized. (f, g) Overlay of the experimental image of acoustic deflection of the sample jet with simulation results. (f) Initial position of the tracer particles before SAW actuation. The particles are aligned along the sample liquid, which, in the absence of acoustic actuation, is confined by the sheath flow to a thin jet along the center of the channel, finally flowing into the waste (bottom) outlet. (g) A 1 ms SAW pulse deflects the jet, driving it upwards, so that it will later flow into the collect (upper) channel. The points denote the simulated deflection of fluid particles which are initially positioned along the undeflected jet at 3 different z-heights: (red) 10 μm above the channel bottom; (green) center; and (blue) 10 μm below channel top. The simulations reproduce the deflection as well as the broadening of the jet due to different deflection velocities along the z-axis. The scalebar denotes 50 μm.

reproduced: the highest velocities are close to the central flow, while the lower velocities appear in the backflow regions, as expected. We qualitatively understand the resultant flow field by considering that the volume force acts only on the region of the post in the middle of the sorting region, creating a pair of vortices, with a flow mainly in the y-direction above the post and a backflow in the $-y$-direction to the left and right of the post to comply with the equation of continuity for the incompressible fluid volume.

Sorting of cells and jet deflection

To directly apply the results of our acoustofluidic simulations to a realistic sorting scenario we study the acoustic streaming effect on the fluid jet of our cell sorting experiment that is used to align cells in the sorting region as shown in

Fig. 4f, g. When the SAW is switched off, the fluid from the sample inlet and the embedded cells travel along a straight trajectory towards the outlet along a jet. This jet is visualized in the microscope by using slightly different solvents for sample and sheath fluid that causes small differences in optical densities. When the SAW is activated, the initial Poiseuille flow is modified by an additional acoustic streaming force. As a result the jet and the embedded cells are deflected. This experimental setup has been simulated by adding pressurized inlets and outlets to the SAW simulations. In the simulations we follow the streamlines of tracer particles which are initially positioned in the center of the channel (parallel to the x-axis) at different z-heights. In Fig. 4 we show the initial position (f) and the position directly after a pulse of 1 ms duration (g) superimposed on the experimental data. There is a good match of both, with the general shape of the jet as

well as the small broadening of the jet width due to different vortex velocities along the *z*-axis.

Materials and methods

Preparation of cells and droplets. For droplet sorting, monodisperse droplets of aqueous solution suspended in an apolar bulk phase were generated using drop makers as described elsewhere.[30,38] As aqueous solutions we used 20 mM bromophenol blue for the non-fluorescent black droplets and 1 mM and 0.3 mM fluorescein solution for the fluorescent droplets. The osmolarity of the solutions was matched by adding sucrose to avert osmotic volume exchange between closely packed droplets. For the apolar bulk phase we used fluorocarbonated oil (3M™ Novec™ Engineered Fluid HFE-7500). To stabilize the surface of the droplets, we added 1% w/v of a PFPE-PEG block copolymer, which is a biocompatible surfactant.[29] The different droplet populations were produced separately and mixed prior to sorting.

For cell sorting we used B16F10 mouse melanoma cells. To enable fluorescence detection, the cells were treated with a fluorescent dye that is sensitive to cell metabolic activity (Calcein-AM, Sigma-Aldrich).[34,35] This preparation yields a cell population with varying fluorescence intensity. The cells were suspended in isosmotic phosphate-buffered saline (PBS) solution. The density of the liquid was matched to the cells by adding density gradient medium (OptiPrep™ Density Gradient Medium, Sigma-Aldrich).

Fabrication of the hybrid device. For the generation of the SAW, we use a transparent piezoelectric substrate (polished, 128° rot, Y-cut LiNbO₃) with a tapered interdigital transducer (T-IDT) with 60 finger pairs. The T-IDT is structured by standard photolithography methods and then metallized by electron beam vapor deposition. Metallization consists of 50 nm gold sandwiched between two 10 nm titan layers used as an adhesion promoter. The chip is then covered with a 200 nm glass layer deposited by a sputtering process to protect the structures from mechanical damage and create a chemically inert barrier.

Due to the tapered design, the periodicity of the IDT varies along its 500 μm long aperture from 23.0 μm to 24.3 μm, corresponding to a resonance frequency of 161 to 171 MHz. The tapered design allows for shaping a thin SAW path[39,40] with a full width at half maximum on the order of 150 μm. By tuning the frequency of the generator, the position of the SAW path can be fine-tuned, allowing for the precise placement of the SAW.

The microfluidic channel has a two-layer PDMS design consisting of a top layer comprising the actual microchannel and a bottom layer consisting of a thin film with the post (or two posts for triple sorting) protruding from the bottom. Both layers were produced using the SU-8 photoresist (NANO™ SU-8 50, MicroChem Corp) on silicon wafers. The top layer is then produced by pouring a 5 mm thick layer of PDMS onto the mold. The bottom film is produced by spinning PDMS on the mold at spin speeds of 2000 rpm for

60 seconds, resulting in a 15 μm thick PDMS layer, with the posts protruding another 15 μm. PDMS is cured at 65 °C for 3 hours. The top layer is subsequently detached from the mold and the inlet and outlet holes are punched using a coring tool (Harris Uni-Core Multi-Purpose Sampling Tool 0.75 mm). The top and bottom layers are treated with ozone plasma for 10 seconds at 100 W to activate the surface. The two layers are immediately brought into contact with a thin ethanol film preventing premature binding. Alignment of the layers is performed manually under a microscope. After 10 minutes of evaporation time, the two PDMS layers are bound and the device can be pulled off the silicon mold.

The PDMS device is then placed on top of the SAW chip, with the PDMS post positioned in front of the IDT along the path of the SAW.

Sorting device and operation. Optical detection is performed with a 473 nm 150 mW DPSS laser focused on the channel. The fluorescence signal of the samples was detected with a photomultiplier tube (Photosensor Module H9858-20, Hamamatsu Photonics, Germany). The signal is analyzed in real time with a custom LabView routine (LabView 2009, National Instruments, Germany) embedded in a field programmable gate array (NI PCI-7833R Virtex-II 3M Gate R, National Instruments, Germany). If the intensity of the fluorescence signal exceeds a preset threshold, a delayed TTL-level pulse is generated and fed into a high-frequency generator (Rohde & Schwarz SMP02) to pulse-modulate its output. The resulting high-frequency pulse is amplified (ZHL-2, Mini-Circuits) and fed to the interdigitated transducer, where it excites a surface acoustic wave (SAW) on the piezo-chip to diverge the sample.

For the triple sorter, additional frequency modulation and two different thresholds are used. If the signal exceeds the lower threshold, a pulse is generated as above. If the signal exceeds the upper threshold, an additional frequency modulation signal is generated and fed to the HF generator. The two frequencies are adjusted to ensure that the SAW generated by the unmodulated signal couples to the left post, and the SAW generated by the modulated signal couples to the right post, resulting in deflection to the top or the bottom outlet, respectively.

Sorter operation was recorded with a microscope (Olympus CKX41) and a high-speed camera (Photron Fastcam 1024 PCI).

Fluidic device setup. The fluidics is driven by syringe pumps (PHD 2000 Infusion, Harvard Apparatus). Typical sample flows are 25 μl h⁻¹. The sheath flow rates are adjusted to ensure that, in the absence of actuation, the particles to be sorted flow into the default channel, but near the edge of the junction, so that they can be easily deflected into the collect channel. Sheath flows are typically in the range of 1000–2000 μl h⁻¹.

Flow field measurements and simulations. For measuring the flow field, a suspension of polystyrene microbeads with a diameter of 2 μm was used (Polybead® Microspheres 2.00 μm, Polysciences Europe). The beads were diluted 1 : 100 v/v with a mixture of 15% v/v OptiPrep and 85% v/v PBS, with

the density of the liquid matched to the bead density to eliminate buoyancy.

The movement of the beads was recorded with a high-speed camera (see above) and analysed with particle image velocimetry.‡

The simulations were done with COMSOL Multiphysics (version 4.2a). A stationary laminar flow of an incompressible fluid was modeled using the full Navier–Stokes equation.

The acoustically generated volume force is calculated from the intensity profile of the SAW on the chip surface. We approximate the profile by assuming unidirectional SAW propagation along the y-direction and interference of the waves excited by single IDT electrode fingers. This results in a typical diffraction profile $I_{SAW}(x) \propto \text{sinc}^2 x/b$ and a half-width of the central maximum $b = 125$ μm. The absolute intensity and the ratio of the SAW diffracted into the PDMS post can be estimated from delay line measurements. Since impedance matching between PDMS and water is very good,[41] practically all of the wave's energy is transmitted into the liquid. Thus, the intensity of the acoustic wave on top of the post is:

$$I_{ac}(x,y) = I_0 \exp\left(-\frac{(y-y_0)}{a_{SAW}}\right) \times \text{sinc}^2(x/b)$$

with the SAW attenuation length $a_{SAW} = 213$ μm and $I_0 = 0.15$ W m^{-2} for an electric signal of 15 dBm and the position of the post edge y_0. Attenuation in water can be neglected because the attenuation length is much higher than the channel height. The propagation direction of the wave (and therefore the direction of the force) is along the yz-plane tilted by a Rayleigh angle of 21.8° with respect to the z axis.

Conclusions

We have introduced a versatile SAW-actuated microfluidic sorter (SAWACS) with sorting rates of 3000 s^{-1} at a moderate acoustic power of 15 dBm. In our acoustic method we gently direct cells into the collect channel. We apply only low shear forces because we switch fluid volumes instead of applying forces directly to the target cell. The amplitude of the electric voltage that we use to excite the acoustic wave on the piezoelectric substrate is lower than 1.8 V at the highest power we used. For such moderate acoustic amplitudes we have demonstrated good cell viability.[42] Because we switch the flow, the method does not require additional responsive particles to enhance sorting. Sorting does not need magnetic or dielectric labeling and can operate in the same way under different physiological conditions as well as on different targets. Unlike electric methods, it is independent of the electrolytic buffer used to suspend the cells. The streaming velocity and sorting speed could be further optimized by using a higher SAW frequency, thus decreasing the attenuation length.[43–45]

‡ JPIV 2.1, Peter Vennemann, www.jpiv.vennemann-online.de.

The sorting rates achieved by our traveling wave device are considerably higher than those achieved by standing wave based devices so far. While these devices can achieve high throughput when separating particles in bulk by size, they report longer switching times[6] and sorting rates of 222 droplets s^{-1}.[10] As the wavelengths in standing wave devices have to be comparable to channel width, optimization by increasing SAW frequency is not possible. Furthermore, the PDMS channel has to be aligned very precisely to the substrate.

When operating the device as a cell sorter, the handling of cells is similar to commercially available FACS machines because it uses single phase flow. Cells that enter from a sample reservoir move through a tube into the interrogation area and are sorted directly from the continuous cell buffer medium into multiple outlet channels based on the level of the fluorescence signal. In this mode our sorter has the same advantage as conventional FACS sorting that does not require additives.

However, our microfluidic sorter has a number of improved capabilities compared to FACS. While FACS requires the dispersion of samples into drops that produce the potential biohazardous aerosol, drop formation is not required for our sorter and the device is fully self-contained. This greatly simplifies the safe handling of biohazardous materials. According to the International Society for Analytical Cytology (ISAC), aerosol production is the most critical and serious issue for biosafety concern.[46] The acoustic platform we suggest avoids this drawback by sorting directly from the continuous single-phase buffer solution. This not only reduces biosafety concerns but also greatly reduces the cost of maintaining and containment of the cell sorting system. Because the chip is disposable it makes elaborate cleaning procedures of the system unnecessary. Furthermore, the absence of drop formation dramatically simplifies optical detection and makes interrogation of the sample more reliable.

The sorter that we have demonstrated is not only limited to cell sorting but can also sort different types of objects independent of their size or physical properties. To show this versatility we have sorted drops of an emulsion. Drops are useful for cell encapsulation and can be loaded with a biological or synthetic cargo. They enhance studies of protein expression of cells and are useful in many ways, for example, for assays and as drug delivery containers. Using drops enables qualitatively new studies in many fields including directed evolution and drug screening. Based on their fluorescence level we were able to demonstrate fast droplet sorting into two and multiple channel outlets at high rates of up to 3000 s^{-1} without any sorting errors.

This rate limit is mainly caused by the occurrence of droplet coalescence above a certain shear stress in the alignment channel. Since this shear stress is proportional to droplet rate, it sets an upper limit to the sorting rate.

However, novel alignment methods like acoustic focusing,[5] which can be easily integrated into the device, do not rely on geometric constraints for alignment and therefore substantially reduce shear stress. In combination with increasing droplet

stability achieved through optimization of droplet surfactants, this coalescence limit can be overcome.

The sorter is also easily integrated into available fluidic platforms and technology. Since our sorting channel device is optically transparent, it can be combined with existing optical flow cytometric detection methods. Applicable SAW-based alignment methods using standing acoustic waves to align cells[6,47] can be simply integrated into our device. By increasing acoustic power, improving droplet alignment and parallelization, our sorter can also be optimized to further increase sorting rate and efficiency even more. In addition, new methods to precisely control the volume of drops with acoustics are straightforward to implement.[48] Furthermore, since our sorter works by fluid switching, it is not only limited to droplets or cells but can also sort any detectable object independent of size. Recent advances on detection in microfluidic systems enable a high-throughput analysis of nanoparticles.[49] In combination with our device, this enables sorting of particularly small objects such as nanoparticles, viruses and bacteria, and even proteins or DNA.

Acknowledgements

Notes and references

1 M. Eisenstein, Cell sorting: Divide and conquer, *Nature*, 2006, **441**, 1179–1185.

2 H. M. Shapiro, *Practical Flow Cytometry. Practical Flow Cytometry*, Wiley-Liss, 2003, vol. 4, p. 542.

3 U. Seger, S. Gawad, R. Johann, A. Bertsch and P. Renaud, Cell immersion and cell dipping in microfluidic devices, *Lab Chip*, 2004, **4**, 148–151.

4 P. Augustsson, C. Magnusson, M. Nordin, H. Lilja and T. Laurell, Microfluidic, label-free enrichment of prostate cancer cells in blood based on acoustophoresis, *Anal. Chem.*, 2012, **84**, 7954–7962.

5 J. Shi, X. Mao, D. Ahmed, A. Colletti and T. J. Huang, Focusing microparticles in a microfluidic channel with standing surface acoustic waves (SSAW), *Lab Chip*, 2008, **8**, 221–223.

6 X. Ding, *et al.*, Standing surface acoustic wave (SSAW) based multichannel cell sorting, *Lab Chip*, 2012, **12**, 4228–4231.

7 M. Wiklund and H. M. Hertz, Ultrasonic enhancement of bead-based bioaffinity assays, *Lab Chip*, 2006, **6**, 1279–1292.

8 S. B. Q. Tran, P. Marmottant and P. Thibault, Fast acoustic tweezers for the two-dimensional manipulation of individual particles in microfluidic channels, *Appl. Phys. Lett.*, 2012, **101**, 114103.

9 O. J. E. Jakobsson, C. Grenvall, M. Nordin, M. Evander and T. Laurell, Acoustic Actuated Fluorescence Activated Sorting of Microparticles, *Lab Chip*, 2014, **14**, 1943–1950.

10 S. Li, *et al.*, An on-chip, multichannel droplet sorter using standing surface acoustic waves, *Anal. Chem.*, 2013, **85**, 5468–5474.

11 X. Hu, *et al.*, Marker-specific sorting of rare cells using dielectrophoresis, *Proc. Natl. Acad. Sci. U. S. A.*, 2005, **102**, 15757–15761.

12 U. Kim and H. T. Soh, Simultaneous sorting of multiple bacterial targets using integrated dielectrophoretic-magnetic activated cell sorter, *Lab Chip*, 2009, **9**, 2313–2318.

13 J. F. Edd, *et al.*, Controlled encapsulation of single-cells into monodisperse picolitre drops, *Lab Chip*, 2008, **8**, 1262–1264.

14 S. Köster, *et al.*, Drop-based microfluidic devices for encapsulation of single cells, *Lab Chip*, 2008, **8**, 1110–1115.

15 J. J. Agresti, *et al.*, Ultrahigh-throughput screening in drop-based microfluidics for directed evolution, *Proc. Natl. Acad. Sci. U. S. A.*, 2010, **107**, 4004–4009.

16 J. Dühnen, J. Stegemann, C. Wiezorek and H. Mertens, A new fluid switching flow sorter, *Histochemistry*, 1983, **77**, 117–121.

17 T. Franke, A. R. Abate, D. A. Weitz and A. Wixforth, Surface acoustic wave (SAW) directed droplet flow in microfluidics for PDMS devices, *Lab Chip*, 2009, **9**, 2625–2627.

18 A. R. Abate, J. J. Agresti and D. A. Weitz, Microfluidic sorting with high-speed single-layer membrane valves, *Appl. Phys. Lett.*, 2010, **96**, 203509.

19 A. Y. Fu, C. Spence, A. Scherer, F. H. Arnold and S. R. Quake, A microfabricated fluorescence-activated cell sorter, *Nat. Biotechnol.*, 1999, **17**, 1109–1111.

20 X. Ding, *et al.*, Surface acoustic wave microfluidics, *Lab Chip*, 2013, **13**, 3626–3649.

21 J. Reboud, *et al.*, Shaping acoustic fields as a toolset for microfluidic manipulations in diagnostic technologies, *Proc. Natl. Acad. Sci. U. S. A.*, 2012, **109**, 15162–15167.

22 G. Destgeer, *et al.*, Adjustable, rapidly switching microfluidic gradient generation using focused travelling surface acoustic waves, *Appl. Phys. Lett.*, 2014, **104**, 023506.

23 J. Reboud, C. Auchinvole, C. D. Syme, R. Wilson and J. M. Cooper, Acoustically controlled enhancement of molecular sensing to assess oxidative stress in cells, *Chem. Commun.*, 2013, **49**, 2918–2920.

24 Y. Bourquin, R. Wilson, Y. Zhang, J. Reboud and J. M. Cooper, Phononic crystals for shaping fluids, *Adv. Mater.*, 2011, **23**, 1458–1462.

25 V. Skowronek, R. W. Rambach, L. Schmid, K. Haase and T. Franke, Particle deflection in a poly(dimethylsiloxane) microchannel using a propagating surface acoustic wave: size and frequency dependence, *Anal. Chem.*, 2013, **85**, 9955–9959.

26 G. Destgeer, K. H. Lee, J. H. Jung, A. Alazzam and H. J. Sung, Continuous separation of particles in a PDMS microfluidic channel *via* travelling surface acoustic waves (TSAW), *Lab Chip*, 2013, **13**, 4210–4216.

27 R. Barnkob, P. Augustsson, T. Laurell and H. Bruus, Acoustic radiation- and streaming-induced microparticle velocities

determined by microparticle image velocimetry in an ultrasound symmetry plane, *Phys. Rev. E: Stat., Nonlinear, Soft Matter Phys.*, 2012, **86**, 056307.

28 L. Wesley, Nyborg Acoustic Streaming, *Physical Acoustics 2B: Properties of polymers and nonlinear acoustics*, 1965.

29 C. Holtze, *et al.*, Biocompatible surfactants for water-in-fluorocarbon emulsions, *Lab Chip*, 2008, **8**, 1632–1639.

30 L.-Y. Chu, A. S. Utada, R. K. Shah, J.-W. Kim and D. A. Weitz, Controllable monodisperse multiple emulsions, *Angew. Chem., Int. Ed.*, 2007, **46**, 8970–8974.

31 L. W. Seymour, *et al.*, Tumour tropism and anti-cancer efficacy of polymer-based doxorubicin prodrugs in the treatment of subcutaneous murine B16F10 melanoma, *Br. J. Cancer*, 1994, **70**, 636–641.

32 L. G. Menon, R. Kuttan and G. Kuttan, Inhibition of lung metastasis in mice induced by B16F10 melanoma cells by polyphenolic compounds, *Cancer Lett.*, 1995, **95**, 221–225.

33 P. Valente, *et al.*, TIMP-2 over-expression reduces invasion and angiogenesis and protects B16F10 melanoma cells from apoptosis, *Int. J. Cancer*, 1998, **75**, 246–253.

34 D. Bratosin, L. Mitrofan, C. Palii, J. Estaquier and J. Montreuil, Novel fluorescence assay using calcein-AM for the determination of human erythrocyte viability and aging, *Cytometry, Part A*, 2005, **66**, 78–84.

35 R. Gatti, *et al.*, Comparison of Annexin V and Calcein-AM as Early Vital Markers of Apoptosis in Adherent Cells by Confocal Laser Microscopy, *J. Histochem. Cytochem.*, 1998, **46**, 895–900.

36 S. Lighthill, Acoustic streaming, *J. Sound Vib.*, 1978(61), 391–418.

37 R. F. W. Coates, *Underwater Acoustic Systems*, Halsted Press, New York, 1989.

38 S. L. Anna, N. Bontoux and H. A. Stone, Formation of dispersions using "flow focusing" in microchannels, *Appl. Phys. Lett.*, 2003, **82**, 364.

39 Y. Bourquin, J. Reboud, R. Wilson and J. M. Cooper, Tuneable surface acoustic waves for fluid and particle manipulations on disposable chips, *Lab Chip*, 2010, **10**, 1898–1901.

40 R. Wilson, *et al.*, Phononic crystal structures for acoustically driven microfluidic manipulations, *Lab Chip*, 2011, **11**, 323–328.

41 D.-S. Lin, X. Zhuang, S. H. Wong, M. Kupnik and B. T. Khuri-Yakub, Encapsulation of Capacitive Micromachined Ultrasonic Transducers Using Viscoelastic Polymer, *J. Microelectromech. Syst.*, 2010, **19**, 1341–1351.

42 T. Franke, S. Braunmüller, L. Schmid, A. Wixforth and D. A. Weitz, Surface acoustic wave actuated cell sorting (SAWACS), *Lab Chip*, 2010, **10**, 789–794.

43 M. Alghane, *et al.*, Scaling effects on flow hydrodynamics of confined microdroplets induced by Rayleigh surface acoustic wave, *Microfluid. Nanofluid.*, 2012, **13**, 919–927.

44 M. Alghane, *et al.*, Frequency effect on streaming phenomenon induced by Rayleigh surface acoustic wave in microdroplets, *J. Appl. Phys.*, 2012, **112**, 084902.

45 M. B. Dentry, L. Y. Yeo and J. R. Friend, Frequency effects on the scale and behavior of acoustic streaming, *Phys. Rev. E: Stat., Nonlinear, Soft Matter Phys.*, 2014, **89**, 13203.

46 I. Schmid, C. Lambert, D. Ambrozak and S. P. Perfetto, Standard safety practices for sorting of unfixed cells, *Current protocols in cytometry editorial board J Paul Robinson managing editor et al.*, 2007, ch. 3, Unit 3.6.

47 Y. Chen, *et al.*, Standing surface acoustic wave (SSAW)-based microfluidic cytometer, *Lab Chip*, 2014, **14**, 916–923.

48 L. Schmid and T. Franke, SAW-controlled drop size for flow focusing, *Lab Chip*, 2013, **13**, 1691–1694.

49 J.-L. Fraikin, T. Teesalu, C. M. McKenney, E. Ruoslahti and A. N. Cleland, A high-throughput label-free nanoparticle analyser, *Nat. Nanotechnol.*, 2011, **6**, 308–313.